A Critical Role of *STAYGREEN*/Mendel's *I* Locus in Controlling Disease Symptom Development during *Pseudomonas syringae* pv *tomato* Infection of Arabidopsis[1][W][OA]

Christy Mecey, Paula Hauck, Marisa Trapp, Nathan Pumplin, Anne Plovanich, Jian Yao, and Sheng Yang He[2]*

Department of Energy Plant Research Laboratory, Michigan State University, East Lansing, Michigan 48824

Production of disease symptoms represents the final phase of infectious diseases and is a main cause of crop loss and/or marketability. However, little is known about the molecular basis of disease symptom development. In this study, a genetic screening was conducted to identify Arabidopsis (*Arabidopsis thaliana*) mutants that are impaired specifically in the development of disease symptoms (leaf chlorosis and/or necrosis) after infection with the bacterial pathogen *Pseudomonas syringae* pv *tomato* (*Pst*) DC3000. An ethyl methanesulfonate-induced Arabidopsis mutant (*no chlorosis1* [*noc1*]) was identified. In wild-type plants, the abundance of chlorophylls decreased markedly after *Pst* DC3000 infection, whereas the total amount of chlorophylls remained relatively unchanged in the *noc1* mutant. Interestingly, *noc1* mutant plants also exhibited reduced disease symptoms in response to the fungal pathogen *Alternaria brassicicola*. Genetic and molecular analyses showed that the nuclear gene *STAYGREEN* (*SGR*; or Mendel's *I* locus) is mutated (resulting in the aspartic acid to tyrosine substitution at amino acid position 88) in *noc1* plants. Transforming wild-type *SGR* cDNA into the *noc1* mutant rescued the chlorosis phenotype in response to *Pst* DC3000 infection. The *SGR* transcript was highly induced by *Pst* DC3000, *A. brassicicola*, or coronatine (COR), a bacterial phytotoxin that promotes chlorosis. The induction of *SGR* expression by COR is dependent on COI1, a principal component of the jasmonate receptor complex. These results suggest that pathogen/COR-induced expression of *SGR* is a critical step underlying the development of plant disease chlorosis.

Tissue chlorosis and necrosis are among the most frequently observed disease symptoms associated with infection by diverse plant pathogens. These disease symptoms generally occur at the late stages of disease, but are highly relevant to agriculture because they cause actual damage to plant tissues, resulting in yield loss and/or poor marketability of crops. Symptomless infection is often associated with benign or symbiotic plant-microbe associations. Despite its importance in disease, the molecular basis of disease chlorosis and necrosis remain poorly understood.

Pseudomonas syringae pv *tomato* (*Pst*) DC3000, the bacterial pathogen used in this study, is well known for causing localized necrosis and diffuse chlorosis in its hosts tomato (*Solanum lycopersicum*) and Arabidopsis (*Arabidopsis thaliana*; Ma and Cuppels, 1991; Whalen et al., 1991; Katagiri et al., 2002). Many virulence genes are needed for *Pst* DC3000 to cause disease, among which two virulence systems have been studied extensively: the type III secretion system and the phytotoxin coronatine (COR). The type III secretion system delivers dozens of effector proteins into plant cells (Alfano and Collmer, 2004; He et al., 2004; Büttner and He, 2009). Many of these effectors suppress host immune responses (Boller and He, 2009; Cui et al., 2009; Lewis et al., 2009) and some are also linked to production of disease necroses (Badel et al., 2003; DebRoy et al., 2004; Cohn and Martin, 2005). COR, a molecular mimic of the plant hormone jasmonate, is not only involved in suppression of host immune responses, but also is important for the development of chlorosis symptoms (Feys et al., 1994; Mittal and Davis, 1995; Bender et al., 1999; Kloek et al., 2001; Brooks et al., 2004, 2005; Block et al., 2005; Melotto et al., 2008b). However, because effector- and COR-deficient bacterial mutants are generally affected in multiple steps of pathogenesis, it is often difficult to determine whether these virulence factors contribute to symptom development directly or indirectly

[1] This work was supported by the Chemical Sciences, Geosciences, and Biosciences Division, Office of Basic Energy Sciences, Office of Science, U.S. Department of Energy (grant no. DE–FG02–91ER20021).

[2] Present address: Department of Energy Plant Research Laboratory, Howard Hughes Medical Institute, Michigan State University, East Lansing, MI 48824.

* Corresponding author; e-mail hes@msu.edu.

The author responsible for distribution of materials integral to the findings presented in this article in accordance with the policy described in the Instructions for Authors (www.plantphysiol.org) is: Sheng Yang He (hes@msu.edu).

[W] The online version of this article contains Web-only data.

[OA] Open Access articles can be viewed online without a subscription.

www.plantphysiol.org/cgi/doi/10.1104/pp.111.181826

through promoting bacterial colonization and/or multiplication.

An alternative approach to elucidate the molecular control of disease symptom production would be to isolate plant mutants that exhibit reduced disease necroses and/or chlorosis in response to pathogen infection. Indeed, numerous Arabidopsis constitutive defense mutants that show no or reduced disease symptoms to *P. syringae* infection have been isolated since the early 1990s (Bowling et al., 1994). However, similar to the situation with effector- or COR-defective *Pst* DC3000 mutants, bacterial populations in such plant mutants are often reduced compared to those in susceptible plants, making it difficult to conclude whether corresponding plant genes have a direct role in mediating symptom development or indirectly through affecting bacterial multiplication. There are a few exceptions: The Arabidopsis mutant *ethylene-insensitive2* and the Arabidopsis mutant *suppressor of G2 allele of skp1* (affected in jasmonate signaling) exhibit reduced disease symptoms to *Pst* DC3000 infection without significantly affecting bacterial growth (Bent et al., 1992; Uppalapati et al., 2011), implicating the involvement of ethylene and jasmonate signaling in the production of *Pst* DC3000-elicited disease symptoms. How ethylene or jasmonate signaling lead to downstream disease symptom is not understood.

To increase our understanding of the molecular basis of disease symptom development during *Pst* DC3000 infection of Arabidopsis, we conducted a genetic screen for Arabidopsis mutants that are reduced in disease symptom development, but not *Pst* DC3000 multiplication. In this article, we report the identification and characterization of such an Arabidopsis mutant and cloning of the corresponding gene. Our results suggest that pathogen-responsive *STAY-GREEN* (*SGR*)/*NON-YELLOWING*/Mendel's *I* locus plays a critical role in controlling disease chlorosis induced by *Pst* DC3000 and, interestingly, also by a fungal pathogen, *Alternaria brassicicola*.

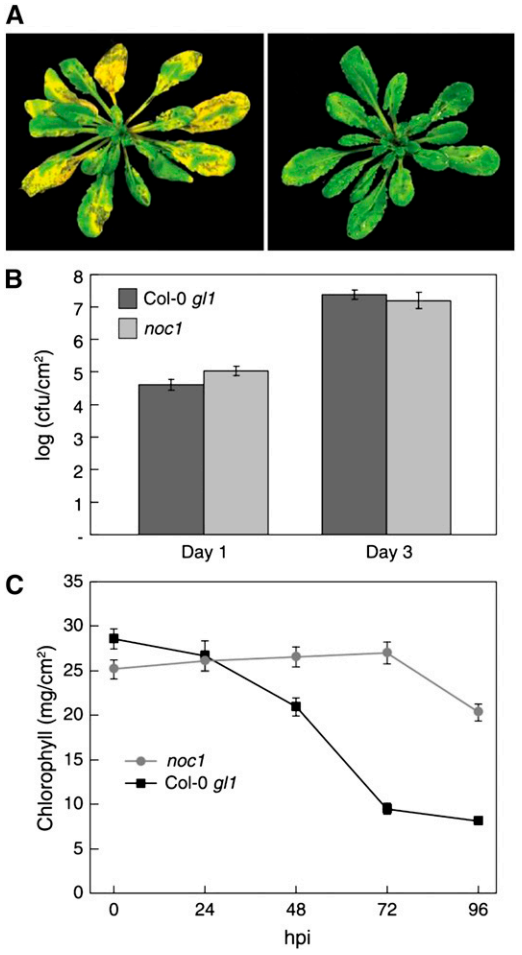

Figure 1. The phenotypes of the *noc1* mutant following *Pst* DC3000 infection. A, Arabidopsis Col-0 *gl1* plant exhibiting typical chlorosis and water-soaking phenotype associated with *Pst* DC300 infection at 72 hpi (left); *noc1* mutants display water soaking but little chlorosis following *Pst* DC3000 infection (right). B, Col-0 *gl1* and *noc1* plants were dip inoculated with *Pst* DC3000 at 10^8 CFU/mL. Bacterial populations were determined at 1 and 3 dpi. C, Chlorophyll amounts in the *noc1* mutant and wild-type Col-0 *gl1* subsequent to *Pst* DC3000 infection at 0, 24, 48, 72, and 96 hpi.

RESULTS

Identification of the *no chlorosis1* Mutant

Approximately 10,000 ethyl methanesulfonate-mutagenized Arabidopsis ecotype Columbia-0 (Col-0) *glabrous1* (*gl1*) plants were screened for altered symptom development after the plants were dipped in a suspension containing 1×10^8 colony forming units (CFU)/mL *Pst* DC3000 bacteria. One mutant isolated from this screen, *no chlorosis1* (*noc1*), was found to be defective in symptom development. In all experiments, *noc1* leaves remained green whereas wild-type leaves began to show chlorosis between 48 and 72 h after inoculation (Fig. 1A). In most experiments reduced severity of necrosis symptom was also observed in *noc1* plants, although this phenotype was not as obvious as the lack-of-chlorosis phenotype. There were no noticeable differences between wild-type and *noc1* plants in size, morphology, growth, or development in the absence of pathogen inoculation. Most importantly, the reduction in disease symptoms in *noc1* plants was not caused by reduced bacterial multiplication because *Pst* DC3000 populations in Col-0 *gl1* and *noc1* plants were similar at 1 and 3 d postinfection (dpi; Fig. 1B). Thus, *noc1* is a bona fide disease symptom mutant.

In addition to the *noc1* mutant, we also isolated several other mutants that exhibited reduced disease symptom development during this study. However, these other mutants were dwarf and/or necrotic, suggestive of constitutive activation of nonspecific disease resistance (Bowling et al., 1994). We did not conduct further characterization of such mutants.

Maintenance of the Chlorophyll Level in *noc1* Plants after Infection with *Pst* DC3000

To quantify the chlorotic response to *Pst* DC3000, we conducted a chlorophyll abundance assay using leaf tissue infiltrated with 2×10^6 CFU/mL of *Pst* DC3000 and collected at 0, 24, 48, 72, and 96 h postinoculation (hpi). The results from one representative experiment are shown in Figure 1C. Prior to inoculation with *Pst* DC3000, *noc1* and wild-type plants had approximately equal amounts of total chlorophyll (25.2 and 28.6 mg/cm^2, respectively). Wild-type plants began to lose chlorophyll by 24 hpi, with levels decreasing through 96 hpi. At 72 hpi, *noc1* plants contained almost 3 times more chlorophyll than wild-type plants (27.0 mg/cm^2 in *noc1* plants versus 9.5 mg/cm^2 in wild-type plants). This experiment demonstrates that wild-type plants lose chlorophyll much faster than *noc1* plants after *Pst* DC3000 infection.

The *noc1* Phenotype Results from a Single Nucleotide Change in *AtSGR1* (At4g22920)

To identify the *NOC1* gene, *noc1* plants were crossed with Landsberg *erecta* (L*er*) plants and the F1 progeny were selfed to create an F2 population for mapping. The *noc1* mutation shows normal Mendelian genetics and is recessive. We initially used bulk segregant analysis to analyze a pool of approximately 100 F2 individuals that exhibited the mutant phenotype (homozygous for the *noc1* mutation). One marker, NGA107, located on the long arm of chromosome 4, showed linkage to the mutation. We tested a larger population of F2 individuals using additional chromosome-4-specific insertion and deletion (INDEL) markers identified from the Monsanto Arabidopsis Polymorphism, L*er* Sequence Collection (St. Louis, MO). This delimited the region of the *noc1* mutation to the area between two INDEL markers (T12H17-13C and F16G20-22) located on chromosome 4 at 11.96 Mb and 12.25 Mb, respectively (Fig. 2A).

Based on the impaired chlorosis phenotype of the *noc1* mutant, we reasoned that the mutation might lie in a gene coding for a chloroplast-targeted protein. The mapped region for the *noc1* mutation includes six genes encoding predicted chloroplast localization signals. The cDNA clones of candidate genes from *noc1* and Col-0 *gl1* plants were subjected to sequencing and revealed a single guanine to thymidine nucleotide mutation, resulting in an Asp (D) to Tyr (Y) amino acid substitution at position 88 of At4g22920/*AtSGR*/*NON-YELLOWING*/Mendel's *I* locus (*AtSGR* hereafter; Fig. 2B). Orthologs of *AtSGR* (Ren et al., 2007) in monocot and dicot species are tightly conserved overall with no variation occurring at this particular residue (Fig. 2C).

To determine whether the D88Y mutation in *AtSGR* is responsible for the *noc1* phenotypes, we transformed *noc1* plants with the full-length *AtSGR* cDNA from Col-0 *gl1* cloned in pBAR-35S, which contains the cauliflower mosaic virus 35S promoter and Basta (glufosinate)-resistance gene. Ten independent T2 lines were confirmed to exhibit Basta resistance and to harbor the *AtSGR* transgene. Three homozygous T3 lines were chosen for disease symptom observations after infection by *Pst* DC3000. In preliminary tests, all three were restored in chlorosis symptom development. We then focused on line 1 for further disease symptom and bacterial growth analyses. Results from this line are shown in Figure 3. By 72 to 96 hpi, *Pst* DC3000-infected *noc1/35S:AtSGR* plants showed disease symptoms, including chlorosis, that were more pronounced than *Pst* DC3000-infected Col-0 *gl1* plants (Fig. 3, A–C). Interestingly, in these experiments we noticed that *noc1/35S:AtSGR* plants did not support bacterial multiplication to the level observed in either *noc1* or Col-0 *gl1* plants at day 3 (Fig. 3E). This observation raised the possibility that accelerated disease symptoms may negatively affect *Pst* DC3000 growth and, accordingly, the *noc1* mutant may allow better bacterial growth. However, we did not observe an enhanced *Pst* DC3000 growth at day 3 in *noc1* plants (Figs. 1B and 4E). We commonly use a 3-d period for assessing *Pst* DC3000 multiplication in the laboratory; however, bacterial infection in the field involves longer durations. We therefore extended our multiplication assay to 6 d, which led to an interesting finding. *Pst* DC3000 populations declined in Col-0 *gl1* and *noc1/35S:AtSGR* plants, as infected tissues senesced, whereas *Pst* DC3000 maintained a high population in the *noc1* plants (Fig. 3E). These results suggest that disease symptom development restricts *Pst* DC3000 persistence in infected tissues.

Effect of the *noc1* Mutation on *A. brassicicola*-Induced Chlorosis

To determine whether *noc1* plants are also affected in disease symptoms caused by a fungal pathogen, Col-0 *gl1* and *noc1* plants were inoculated with spores of the necrotrophic fungus *A. brassicicola*. A necrotic lesion developed at the site of inoculation in Col-0 *gl1*, *noc1*, and complemented *noc1/35S:AtSGR* plants at 5 to 10 dpi. In some experiments, a chlorotic halo, surrounding the necrotic lesion, may also develop within 5 to 10 dpi in only Col-0 *gl1* and *noc1/35S:AtSGR* plants (Fig. 4A). However, the chlorosis phenotype induced by *A. brassicicola* was variable between experiments and could not be quantified reproducibly. To quantify disease symptoms, we therefore measured necrotic lesion areas using ImageJ software. The area of necrotic lesion development was smaller in *noc1* plants infected with *A. brassicicola* than that in Col-0 *gl1* plants infected in the same manner (Fig. 4). Fungus-induced disease necroses were restored in *noc1/35S:AtSGR* plants infected with *A. brassicicola* (Fig. 4). Plants inoculated with buffer control (0.1% Tween 20) alone showed no signs of chlorosis or necroses (Fig. 4A). These results demonstrate that *AtSGR1* is required for the development of disease symptoms caused by a necrotrophic pathogen.

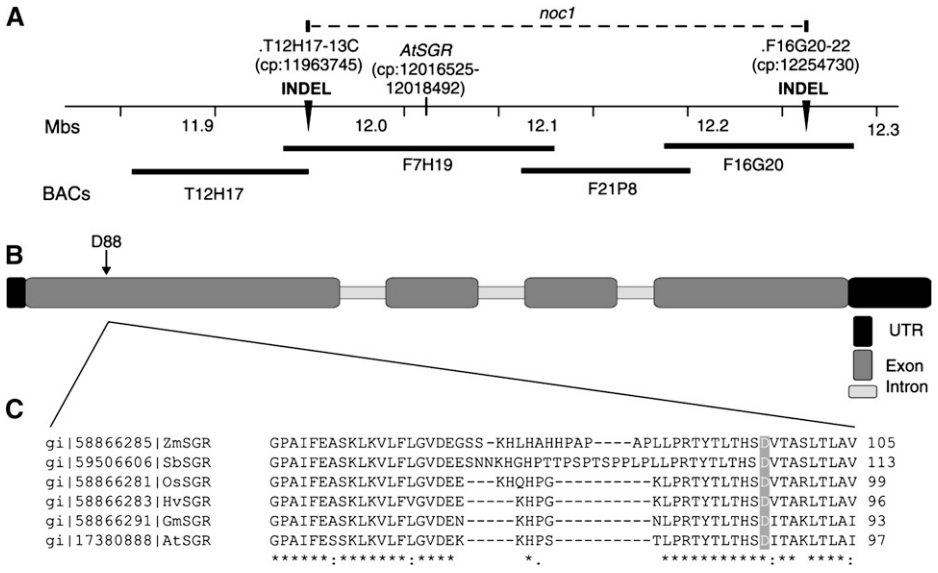

Figure 2. Map-based identification of the *noc1* mutation. A, A portion of the long arm of Arabidopsis chromosome 4 where the *noc1* mutation is located between the two INDEL markers (T12H17-13C and F16G20-22; indicated by black arrowheads) at chromosomal positions (cp) 11963745 and 12254730, respectively. B, Gene structure of *AtSGR* (At4g22920; cp: 12016525–12018492), showing the location of the *noc1* mutation, an Asp to Tyr substitution at position 88 resulting from a guanine to thymidine nucleotide mutation. C, The residue D88 is conserved among *SGR* orthologs in diverse plants, including *Zea mays* (gi 58866285), *Sorghum bicolor* (gi 59506606), *Oryza sativa* (gi 58866281), *Hordeum vulgare* (gi 58866283), and *Glycine max* (gi 58866291). Orthologous sequences were arranged using CLUSTALW software.

AtSGR Is Highly Induced during *Pst* DC3000 and *A. brassicicola* Infection

Previous studies have shown that *SGR* expression is critical for initiation of developmentally regulated chlorophyll degradation in a number of plant species (Armstead et al., 2006, 2007; Park et al., 2007; Ren et al., 2007). The requirement of *AtSGR* for disease chlorosis suggests that the expression of *AtSGR* might be induced during pathogen infection. To examine this possibility, we collected total RNA from water- and *Pst* DC3000-inoculated *noc1* and Col-0 *gl1* plants at 36, 48, and 60 hpi and performed northern-blot analyses using an *AtSGR*-specific probe. We found that the *AtSGR* expression is strongly induced by *Pst* DC3000, but not water, in both Col-0 *gl1* and *noc1* plants at all sampled time points (Fig. 5A). Thus, *AtSGR* expression is regulated during *Pst* DC3000 infection and the *noc1* mutation does not significantly affect this expression. Quantitative reverse transcription (RT)-PCR analysis was also performed with RNA from *A. brassicicola*-infected leaves, showing that *AtSGR* expression was induced by fungal infection (Fig. 5B; Supplemental Fig. S1).

We next investigated whether specific virulence factors of *Pst* DC3000 could induce the expression of *AtSGR*. COR is a well-known bacterial virulence factor that promotes the development of disease chlorosis in plants (Uppalapati et al., 2005, 2007; Ishiga et al., 2009). Recent studies have demonstrated that COR mimics the active form of the plant hormone jasmonate and directly targets the jasmonate receptor complex in which the CORONATINE INSENSITIVE1 (COI1) F-box protein is a principal component (Katsir et al., 2008; Melotto et al., 2008a; Fonseca et al., 2009; Sheard et al., 2010). To determine whether COR could induce expression of *AtSGR*, we treated 8-d-old, Col-0 *gl1* seedlings with buffer or 10 μM COR. Seedlings were collected at 3 h posttreatment and total RNA was isolated for each group. Quantitative RT-PCR analysis showed that, like *JAZ9* (a known COR/jasmonate-responsive gene; Thines et al., 2007), *AtSGR* expression was induced by COR (Fig. 6A; Supplemental Fig. S2A). We next examined whether COR-induced expression of *AtSGR* requires COI1-dependent jasmonate signaling. As shown in Figure 6A, COR could not induce *AtSGR* expression in the *coi1* mutant (Feys et al., 1994). These results suggest that COR induction of *AtSGR* expression requires an intact jasmonate signaling pathway.

Finally, we examined whether COR production is necessary for *Pst* DC3000 to induce the expression of *AtSGR*. Col-0 *gl1* plants were infected with *Pst* DC3000 or a COR-deficient mutant strain, DB29 (Uppalapati et al., 2007). Quantitative RT-PCR analysis revealed that expression of *AtSGR* is strongly induced by 48 hpi, continuing through 72 hpi, in Col-0 *gl1* plants infected with either DB29 or *Pst* DC3000 (Fig. 6B; Supplemental Fig. S2B), although expression of *AtSGR* was significantly higher in plants infected with DC3000 as compared to those infected with DB29. These data indicate that COR is sufficient but not

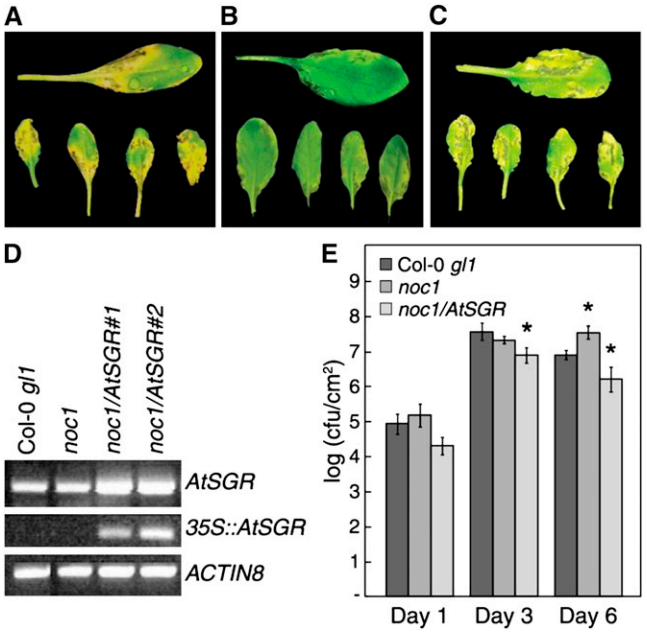

Figure 3. Complementation of the *noc1* mutation by 35S:*AtSGR*. Disease symptoms on Col-0 *gl1* (A), *noc1* (B), and *noc1*/35S:*AtSGR* line 1 (C) leaves 4 d after dip inoculation with *Pst* DC3000 at 1×10^8 CFU/mL. D, RT-PCR using *AtSGR*-specific primers showing native expression of endogenous *AtSGR* in Col-0 *gl1* and *noc1* plants and increased expression in *noc1* lines complemented with *35S:AtSGR* transgene (top). RT-PCR using primers utilizing transgene-specific primers (see "Materials and Methods") shows expression of *35S:AtSGR* only in complemented *noc1* lines (middle). RT-PCR of *ACTIN8* was used as a loading reference (bottom). E, *Pst* DC3000 multiplication assay. Col-0 *gl1*, *noc1*, and *noc1*/*AtSGR* plants (line 1) were dip inoculated with *Pst* DC3000 at 10^8 CFU/mL. Bacterial populations were determined at 1, 3, and 6 dpi. *t* tests were performed in Microsoft Excel using a two-sample, equal variance formula. Comparisons are between Col-0 *gl1* and *noc1* and between Col-0 *gl1* and *noc1*/*AtSGR* at each time point. *P* values of <0.05 are indicated with a single asterisk (*).

necessary for *Pst* DC3000 to induce *AtSGR* expression during infection.

DISCUSSION

Development of disease symptoms represents the final stage of a pathogenic infection and is particularly destructive to the plant because it damages plant tissues, affecting not only crop productivity, but also crop marketability. Reduced disease symptoms, in the form of disease-tolerant cultivars, could be exploited as a method of disease management. Despite its importance in disease, the molecular control of disease symptom production remains one of the least-understood aspects of plant diseases.

Although ethylene and jasmonate signaling pathways are known to be important for *Pst* DC3000-induced disease chlorosis (Bent et al., 1992; Uppalapati et al., 2011), it is not understood how these pathways ultimately impact chlorophyll homeostasis in infected tissues. Our isolation of the *noc1* mutant and subsequent identification of *AtSGR* gene begin to provide molecular insight into how *Pst* DC3000 infection perturbs chlorophyll homeostasis and causes tissue chlorosis. Previous research has suggested that SGR-family proteins, once produced during senescence, enter the chloroplast and destabilize photosystem complexes, which seems to be a prerequisite for regulated chlorophyll degradation (Park et al., 2007). We found that *Pst* DC3000 infection induces the expression of *AtSGR* and transgenic constitutive expression of *AtSGR* accelerates disease symptom development caused by *Pst* DC3000 infection. These results indicate that pathogen-induced disease chlorosis results from

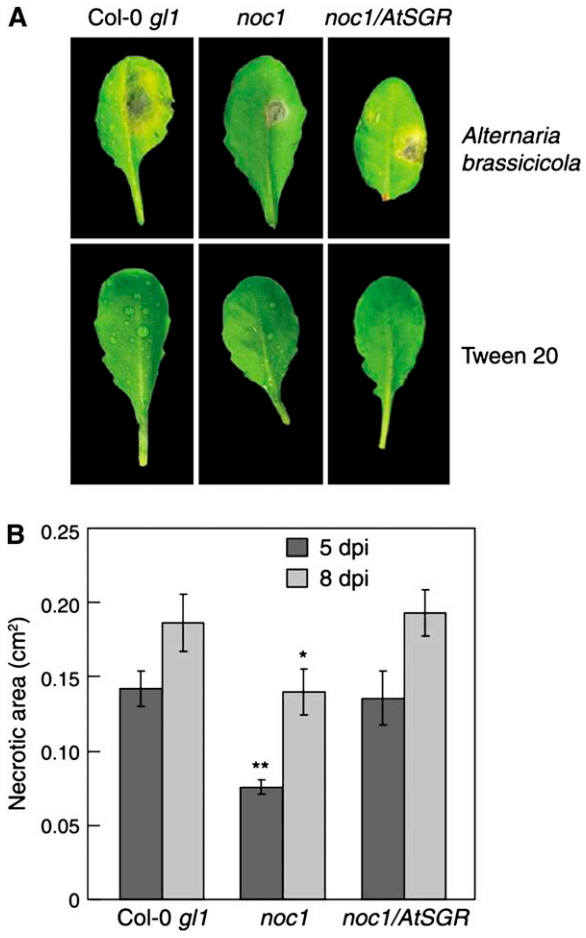

Figure 4. Effects of the *noc1* mutation on *A. brassicicola*-induced disease symptoms. A, Top sections: Chlorosis and/or necrosis caused by *A. brassicicola* infection in Col-0 *gl1* (left), the *noc1* mutant (center), and *noc1*/*35S:AtSGR* (right) leaves 8 dpi. Bottom sections: Mock inoculations with 0.1% Tween 20 are shown. B, Necrotic lesion areas were measured at 5 and 8 dpi in *A. brassicicola*-infected Col-0 *gl1*, *noc1*, and *noc1*/*AtSGR* plants using ImageJ software. Student's *t* tests were performed in Microsoft Excel using a two-sample, equal variance formula. Comparisons are between Col-0 *gl1* and the *noc1* mutant and between Col-0 *gl1* and *noc1*/*35S:SGR* at each time point. *P* values of <0.05 are indicated with a single asterisk (*); *P* values < 0.005 are indicated by **.

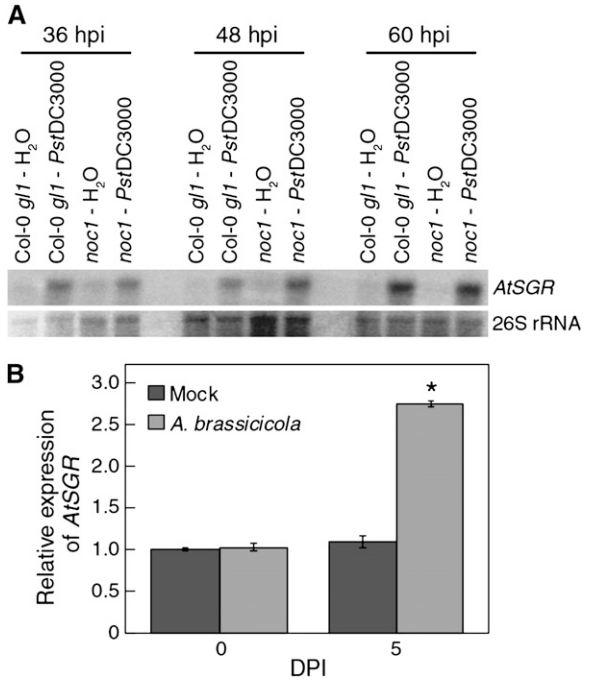

Figure 5. Induction *of AtSGR* expression during infection. A, Northern-blot analysis of *AtSGR* expression in *Pst* DC3000-infected Col-0 *gl1* and *noc1* mutant plants. 26S rRNA visualized by ethidium bromide staining was used as a loading reference. B, Quantitative RT-PCR analysis of *AtSGR* expression in mock- and *Alternaria*-infected Col-0 *gl1* plants at 0 and 5 dpi. Error bars represent SDS from three biological replicates. The experiment was repeated once and similar results were obtained. Asterisks indicate significant difference ($P < 0.05$) between mock- and *Alternaria*-infected Col-0 *gl1* plants using the Student's *t* test.

activation of a key regulator of an endogenous, senescence-associated chlorophyll degradation program.

The identification and characterization of the *noc1* mutant also raises several important issues regarding the relationship between disease symptom development and bacterial pathogenesis. First, our data show that, in the case of *Pst* DC3000 infection at the inoculums of 1×10^6 CFU/mL, the bacterial population reaches a maximum level at 3 dpi in both wild-type and *noc1* plants. However, whereas the *Pst* DC3000 population declined in wild-type Col-0 *gl1* plants, it persisted at a high level for a longer time in *noc1* mutant plants (Fig. 3). This finding has significant ramifications in terms of the role of disease symptom in bacterial pathogenesis. Disease symptoms are commonly believed to be a consequence of collateral damages caused by infection. However, our result suggests that this may not be the case: Disease symptom development can play an active role in negatively impacting the persistence of hemibiotrophic pathogens like *Pst* DC3000 at late stages of pathogenesis. Interestingly, a similar result was observed in the study of XopD, a type III effector of *Xanthomonas campestris* pv *vesicatoria*, which delays symptom development and tissue degeneration in tomato via modulation of host transcriptional programming, resulting in increased pathogen multiplication (Kim et al., 2008).

Second, previous reports show that bacterial phytotoxin COR induces chlorosis in plants and that COR-deficient mutants have reduced ability to cause chlorosis (Ma and Cuppels, 1991; Whalen et al., 1991;

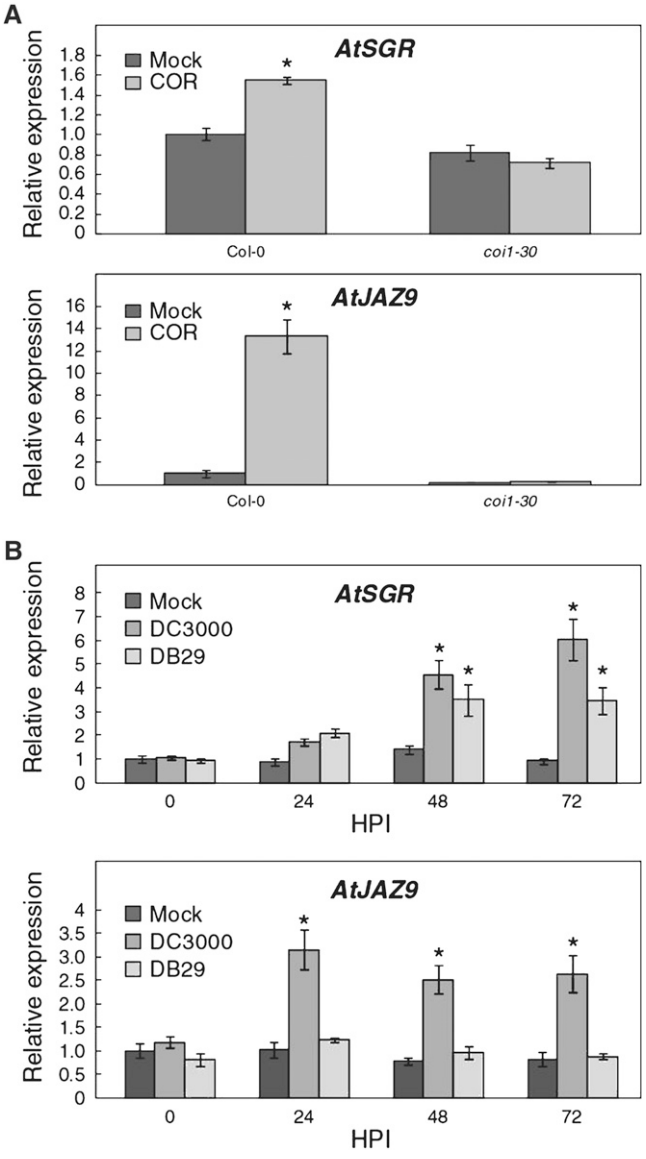

Figure 6. Role of COR in the induction *AtSGR* expression. A, Quantitative RT-PCR showing *AtSGR* and *AtJAZ9* expression in mock- and COR-treated wild-type and *coi1* background plants. Error bars represent SD from three biological replicates. B, *AtSGR* expression is induced by 48 hpi in Col-0 *gl1* plants infected with *Pst* DC3000 (COR^+) or DB29 (COR^-). Quantitative RT-PCR shows At*SGR* and At*JAZ9* expression in mock- and *P. syringae*-infected Col-*gl1* plants. Error bars represent SDS from three biological replicates. Experiments were repeated once and similar results were obtained. Asterisks indicate significant difference ($P < 0.05$) when comparing bacterial infections to mock inoculations using the Student's *t* test.

Uppalapati et al., 2005, 2007). Consistent with these observations, we found that COR was sufficient to activate *AtSGR* expression, providing a molecular basis for the involvement of COR in disease chlorosis. Additionally, COR-treated *coi1* mutants showed no induction of *AtSGR* expression (Fig. 6), suggesting that the jasmonate receptor complex is required for COR-induced expression of *AtSGR*. Interestingly, we found a putative MYC2-binding motif (ACGTG; Boter et al., 2004; Yadav et al., 2005) in the promoter region of *AtSGR* at nucleotide position −23 (data not shown). MYC2 is a major transcription factor involved in jasmonate/COR-induced gene expression (Lorenzo et al., 2004; Laurie-Berry et al., 2006), further suggesting an involvement of jasmonate signaling in COR-mediated induction of *AtSGR* expression. It should be pointed out, however, that in Arabidopsis, purified COR was shown to induce purpling, instead of chlorosis (Bent et al., 1992). The exact reason for this phenomenon is not known. Because COR structurally and functionally mimics jasmonate, which is known to induce anthocyanin production in Arabidopsis (Ellis and Turner, 2001), it is possible that the chlorosis induced by COR in Arabidopsis is masked by purpling associated with anthocyanin production. In any case, although COR is sufficient for induction of *AtSGR*, we found that it is not required for *AtSGR* induction during infection with *Pst* DC3000 (Fig. 6). Thus, it is likely that COR is not the only virulence factor in *Pst* DC3000 that is involved in the development of disease chlorosis, but that the action of additional virulence factors (possibly type III effectors) may also be involved in the induction of *AtSGR* and contribute to the production of disease chlorosis. Indeed, disease chlorosis is often observed in Arabidopsis mutants that allow high multiplication of COR-deficient *Pst* DC3000 (Melotto et al., 2006; Zeng and He, 2010).

Third, in addition to affecting disease chlorosis, the *noc1* mutation also reduced disease necrosis caused by *Pst* DC3000 and *A. brassicicola* infection, although this effect is less obvious compared to that of disease chlorosis (Figs. 1 and 4). This is an interesting finding in light of a recent study that investigated the effect of *AtSGR* overexpression and RNAi-mediated suppression on the hypersensitive response (HR) elicited by *Pst* DC3000 (*avrRpm1*) in Arabidopsis (Mur et al., 2010). It was found that increased and decreased *AtSGR* expression, respectively, accelerated and suppressed the kinetics of HR-associated cell death in resistant Arabidopsis plants. Mur and colleagues postulate that some phototoxic chlorophyll catabolites contribute to HR cell death in resistant plants (Mur et al., 2010). If so, we speculate that such chlorophyll catabolites could also contribute to the formation of disease necrosis in susceptible Arabidopsis plants infected by *Pst* DC3000 or *A. brassicicola*, as observed in our study (Figs. 1 and 4).

The stay-green phenotype was first described in 1866 by Gregor Mendel in differentiating yellow and green cotyledon color in segregating populations of pea (*Pisum sativum*; Mendel, 1866). *SGR* orthologs have been cloned from a wide range of dicot and monocot species (Armstead et al., 2006, 2007; Jiang et al., 2007; Park et al., 2007; Sato et al., 2007; Aubry et al., 2008; Barry et al., 2008). Consequently, we hypothesize that pathogen induction of *SGR* genes may be a common mechanism underlying disease chlorosis across a wide spectrum of plant-pathogen interactions. As such, further study of *SGR* genes and their regulation could lead to transgenic plants with not only controlled senescence, but also disease symptom expression, thereby benefiting agriculture.

MATERIALS AND METHODS

Plant Material, Mutagenesis, and Growth Conditions

Approximately 1 g of Arabidopsis (*Arabidopsis thaliana*) ecotype Col-0 *gl1* seeds was mixed with 100 mL of distilled water and 250 μL of ethyl methanesulfonate. The mixture was incubated overnight at room temperature in the dark with gentle agitation. The seeds were washed six times with 500 mL of distilled water, resuspended in 300 mL of 0.1% agarose, and sown onto a soil mixture (equal portions of Baccto high-porosity professional plant mix, perlite, and vermiculite, covered with a thin layer of fine vermiculite). The flats were covered with lids and incubated in the dark at 4°C for 3 d. The flats were then transferred to a growth chamber (20°C with 12 h of fluorescent light [100 μE m^{-2} s^{-1}] and 12 h of darkness). The plants were self fertilized to create a population of M2 plants.

Screening and Isolation of Arabidopsis Mutants

Four- to 6-week-old M2 plants were dipped in a 1×10^8 CFU/mL suspension of *Pst* DC3000 and 0.05% Silwet L-77 (Lehle Seeds, www.arabidopsis.com) for 2 to 3 s. The inoculated plants were incubated in high (80%–90%) humidity conditions for 96 h and screened for a lack of symptom development.

Bacteria Enumeration in Inoculated Leaves of *noc1* Mutants and Wild-Type Col-0 *gl1* Plants

Four- to 5-week-old plants were used for bacteria enumeration. *Pst* DC3000 was grown in low-salt Luria-Bertani broth to the mid-to-late logarithmic phase at 28°C. Bacterial cultures were pelleted and resuspended in sterile water to a final OD_{600} of 0.2 (equivalent to 1×10^8 CFU/mL) for dip inoculation. Fully expanded leaves were dip inoculated with bacterial suspensions. Plants were placed in trays with standing water and covered with plastic wrap to maintain high humidity. During the experimental period there was no obvious tissue desiccation in inoculated plants. Bacteria enumeration followed the protocol described by Katagiri et al. (2002). *P* values were derived from multiplication data utilizing Microsoft Excel software for *t* test statistical analysis.

Alternaria brassicicola Infection

We inoculated 10 leaves of each plant with 10 μL of *Alternaria brassicicola* spores at a concentration of 6.4×10^5 spores/mL suspended in 0.1% Tween 20. For control inoculations we used 0.1% Tween 20. Plants were covered with humidity domes and kept at high humidity throughout the infection process.

For quantification of disease symptoms caused by fungal infection, the areas of necrotic lesions caused by *Alternaria* inoculation were measured on 30 infected plant leaves. The average lesion area was calculated from 30 to 50 lesions at 5 and 8 dpi using ImageJ software. Older leaves were excluded from the sample set to avoid senescence-associated chlorosis and necrosis.

AtSGR expression was measured in *A. brassicicola*-infected tissue at 0 and 5 dpi. RNA was isolated from leaf tissue using an RNAeasy kit (Qiagen,

www.qiagen.com). Semiquantitative RT-PCR was performed as described by the manufacturer (Takara, www.takara-bio.com).

Chlorophyll Extraction and Quantification

For chlorophyll abundance assays we infiltrated leaf tissue with 2×10^6 CFU/mL *Pst* DC3000 and collected samples at 0, 24, 48, 72, and 96 hpi. All chlorophyll extraction steps were conducted in near darkness. Leaf disks from four separate leaves at each time point were frozen in liquid nitrogen and stored at 80°C. The frozen tissue was homogenized in 600 μL of 80% acetone, the homogenates were centrifuged at 500*g* for three minutes at 4°C, and the supernatant was transferred to a new tube and kept on ice. The absorbance of four dilutions (1:10, 1:5, 1:3, and 1:2.5) of each sample was determined using a spectrophotometer. The amount of chlorophyll was calculated as previously described (Arnon, 1949).

Gene Mapping

Mapping of the *noc1* mutation was conducted as described by Lukowitz and colleagues (Lukowitz et al., 2000). Initial genome-wide screening was conducted using an array of primers (Invitrogen, www.invitrogen.com) to detect simple sequence length polymorphisms from each chromosome. Additional INDELs, identified in the Monsanto Arabidopsis polymorphism and L*er* sequence collection (www.arabidopsis.org/browse/Cereon/index.jsp), were used to further define the region containing the *noc1* mutation (Jander et al., 2002).

Amino acid sequences of *AtSGR* and its orthologs were aligned using ClustalW (www.ddbj.nig.ac.jp/search/clustalw-j.html) and were then adjusted manually. Complementation of the *noc1* phenotype was accomplished by transforming *noc1* plants with 35S:*AtSGR* (At4g22920) in binary vector pBAR-35S (provided by J. Dangl, University of North Carolina, Chapel Hill, NC). The cDNA was amplified from a pool of total Col-0 *gl1* RNA using LA *Taq* polymerase (Takara) and *AtSGR*-specific primers carrying *Xho*I (5′) and *Spe*I (3′) restriction sites (F: ggctcgagatgtgtagtttgtcggc and R: ggactagtctagagtttctccggatt) to facilitate eventual cloning into pBAR-35S. The PCR product was first cloned into pTOPO 2.1 (Invitrogen) and the *AtSGR* insert sequenced. The sequence-verified *AtSGR* insert was then transferred into the *Xho*I and *Spe*I sites of the binary vector pBAR-35S. Plant transformation was conducted as described (Clough and Bent, 1998). Transformants were screened in the T1 and T2 generations for Basta herbicide resistance and in T2 and T3 generations for the presence of the *AtSGR* transgene using RT-PCR with primers specific to the 5′ and 3′ untranslated regions (pBAR1 vector sequence) of the transgene: F-ggattgatgtgatatctccac and R-caagaccggcaacaggattc.

Northern Blotting

For northern-blotting analysis, total RNA was isolated from Arabidopsis leaves using the RNAgents total RNA isolation system (Promega, www.promega.com). The RNA concentration was determined based on A_{260}, and RNA was separated on 2% formaldehyde agarose gels. The RNA was blotted onto Hybond N+ nylon membranes (Amersham, www.gelifesciences.com) using 10× saline sodium citrate buffer and UV cross-linked using a Stratalinker (Stratagene, www.genomics.agilent.com) with the auto-cross-link setting. Approximately 100 ng of a 300-bp exon-coding fragment, from *AtSGR* cDNA, was amplified by PCR using the following primers: F: atgtgtagtttgtcggcgat and R: cccggtatagcctatttgcc. The resulting fragment was purified using the Qiagen gel extraction kit (Qiagen) and labeled with ^{32}P-CTP using random hexamers. Blotted membranes were hybridized with labeled probes using PerfectHyb plus hybridization buffer (Sigma-Aldrich, www.sigmaaldrich.com), following the manufacturer's protocol, and then washed in 0.5× saline sodium citrate buffer and exposed to x-ray film for approximately 16 h.

Quantitative RT-PCR

Total RNAs were isolated from Arabidopsis leaves using the RNAgents total RNA isolation system (Promega, www.promega.com). Poly d(T) cDNA was prepared from 500 ng total RNA using Moloney murine leukemia virus reverse transcriptase (Invitrogen) and quantified on an ABI7500 fast RT-PCR system (Applied Biosystems) with the fast SYBR green master kit (Applied Biosystems) according to the manufacturer's protocols. Expression levels were normalized to *AtPP2AA3* (*PROTEIN PHOSPHATASE 2A SUBUNIT A*, At1g13320; Czechowski et al., 2005). The primers used for RT-PCR were: *AtSGR*, 5′-ACTACCTGTGGTGTTGAAGG-3′ and 5′-CGACTTTGTTGAACTCATTGAC-3′, *AtPP2AA3*, 5′-GGTTACAAGACAAGGTTCACTC-3′ and 5′-CATTCAGGACCAAACTCTTCAG-3′, and *AtJAZ9* (At1g70700), 5′-ATGAGGTTAACGATGATGCTG-3′ and 5′-CTTAGCCTCCTGGAAATCTG-3′.

Induction of *AtSGR* Expression by COR

Arabidopsis seeds (Col-0 *gl1* and *coi1*) were germinated and grown on Murashige and Skoog agar plates for 4 d with *coi1* seedlings being selected on 10 μM methyl jasmonate (Sigma-Aldrich). Seedlings were transferred to fresh Murashige and Skoog plates and grown for another 4 d and were treated with 10 μM COR (Sigma-Aldrich) or 0.1% ethanol by spraying. Seedlings were harvested at 3 h posttreatment and total RNA was isolated using the RNeasy plant mini kit (Qiagen) per manufacturer's instructions. cDNA synthesis of *AtSGR*, *JAZ9*, and *UBC* was completed using avian reverse transcriptase and oligo-DT primers followed by RT-PCR using gene-specific primers (*AtSGR*: F: 5′atgtgtagtttgtcggcgat3′ and R: 5′ctagagtttctccggatttg3′; *JAZ9*: F: 5′atggaaagagattttctgggtttg3′ and R: 5′ttatgtaggagaagtagaagagta3′; *UBC21*: F: 5′tcaaatggaccgctcttatc3′ and R: 5′cacagactgaagcgtccaag3′).

Supplemental Data

The following materials are available in the online version of this article.

Supplemental Figure S1. Semiquantitative RT-PCR analysis of *AtSGR* expression in *Alternaria*-infected Col-0 *gl1*, the *noc1* mutant, and *noc1*/*AtSGR* plants at 0 and 5 dpi.

Supplemental Figure S2. A, Semiquantitative RT-PCR showing levels of expression for *AtSGR* and *JAZ9* in Col-0 seedlings 3 h after treatment with 10 μM COR (+) or buffer (−).

ACKNOWLEDGMENTS

We thank Wanessa Wight and the laboratory of Jonathan Walton for providing *A. brassicicola* spores and Natasha Raikhel for the initial mapping primer set from Invitrogen.

Received June 16, 2011; accepted September 29, 2011; published October 12, 2011.

LITERATURE CITED

Alfano JR, Collmer A (2004) Type III secretion system effector proteins: double agents in bacterial disease and plant defense. Annu Rev Phytopathol **42:** 385–414

Armstead I, Donnison I, Aubry S, Harper J, Hörtensteiner S, James C, Mani J, Moffet M, Ougham H, Roberts L, et al (2006) From crop to model to crop: identifying the genetic basis of the staygreen mutation in the *Lolium*/*Festuca* forage and amenity grasses. New Phytol **172:** 592–597

Armstead I, Donnison I, Aubry S, Harper J, Hörtensteiner S, James C, Mani J, Moffet M, Ougham H, Roberts L, et al (2007) Cross-species identification of Mendel's I locus. Science **315:** 73

Arnon DI (1949) Copper enzymes in isolated chloroplasts: polyphenoloxidase in *Beta vulgaris*. Plant Physiol **24:** 1–15

Aubry S, Mani J, Hörtensteiner S (2008) Stay-green protein, defective in Mendel's green cotyledon mutant, acts independent and upstream of pheophorbide a oxygenase in the chlorophyll catabolic pathway. Plant Mol Biol **67:** 243–256

Badel JL, Nomura K, Bandyopadhyay S, Shimizu R, Collmer A, He SY (2003) *Pseudomonas syringae* pv. *tomato* DC3000 HopPtoM (CEL ORF3) is important for lesion formation but not growth in tomato and is secreted and translocated by the Hrp type III secretion system in a chaperone-dependent manner. Mol Microbiol **49:** 1239–1251

Barry CS, McQuinn RP, Chung MY, Besuden A, Giovannoni JJ (2008)

Amino acid substitutions in homologs of the STAY-GREEN protein are responsible for the green-flesh and chlorophyll retainer mutations of tomato and pepper. Plant Physiol **147:** 179–187

Bender CL, Alarcón-Chaidez F, Gross DC (1999) *Pseudomonas syringae* phytotoxins: mode of action, regulation, and biosynthesis by peptide and polyketide synthetases. Microbiol Mol Biol Rev **63:** 266–292

Bent AF, Innes RW, Ecker JR, Staskawicz BJ (1992) Disease development in ethylene-insensitive *Arabidopsis thaliana* infected with virulent and avirulent *Pseudomonas* and *Xanthomonas* pathogens. Mol Plant Microbe Interact **5:** 372–378

Block A, Schmelz E, Jones JB, Klee HJ (2005) Coronatine and salicylic acid: the battle between Arabidopsis and *Pseudomonas* for phytohormone control. Mol Plant Pathol **6:** 79–83

Boller T, He SY (2009) Innate immunity in plants: an arms race between pattern recognition receptors in plants and effectors in microbial pathogens. Science **324:** 742–744

Boter M, Ruíz-Rivero O, Abdeen A, Prat S (2004) Conserved MYC transcription factors play a key role in jasmonate signaling both in tomato and Arabidopsis. Genes Dev **18:** 1577–1591

Bowling SA, Guo A, Cao H, Gordon AS, Klessig DF, Dong X (1994) A mutation in *Arabidopsis* that leads to constitutive expression of systemic acquired resistance. Plant Cell **6:** 1845–1857

Brooks DM, Bender CL, Kunkel BN (2005) The *Pseudomonas syringae* phytotoxin coronatine promotes virulence by overcoming salicylic acid-dependent defences in *Arabidopsis thaliana*. Mol Plant Pathol **6:** 629–639

Brooks DM, Hernández-Guzmán G, Kloek AP, Alarcón-Chaidez F, Sreedharan A, Rangaswamy V, Peñaloza-Vázquez A, Bender CL, Kunkel BN (2004) Identification and characterization of a well-defined series of coronatine biosynthetic mutants of *Pseudomonas syringae* pv. *tomato* DC3000. Mol Plant Microbe Interact **17:** 162–174

Büttner D, He SY (2009) Type III protein secretion in plant pathogenic bacteria. Plant Physiol **150:** 1656–1664

Clough SJ, Bent AF (1998) Floral dip: a simplified method for *Agrobacterium*-mediated transformation of *Arabidopsis thaliana*. Plant J **16:** 735–743

Cohn JR, Martin GB (2005) *Pseudomonas syringae* pv. *tomato* type III effectors AvrPto and AvrPtoB promote ethylene-dependent cell death in tomato. Plant J **44:** 139–154

Cui H, Xiang T, Zhou JM (2009) Plant immunity: a lesson from pathogenic bacterial effector proteins. Cell Microbiol **11:** 1453–1461

Czechowski T, Stitt M, Altmann T, Udvardi MK, Scheible W-RD (2005) Genome-wide identification and testing of superior reference genes for transcript normalization in Arabidopsis. Plant Physiol **139:** 5–17

DebRoy S, Thilmony R, Kwack YB, Nomura K, He SY (2004) A family of conserved bacterial effectors inhibits salicylic acid-mediated basal immunity and promotes disease necrosis in plants. Proc Natl Acad Sci USA **101:** 9927–9932

Ellis C, Turner JG (2001) The *Arabidopsis* mutant *cev1* has constitutively active jasmonate and ethylene signal pathways and enhanced resistance to pathogens. Plant Cell **13:** 1025–1033

Feys B, Benedetti CE, Penfold CN, Turner JG (1994) *Arabidopsis* mutants selected for resistance to the phytotoxin coronatine are male sterile, insensitive to methyl jasmonate, and resistant to a bacterial pathogen. Plant Cell **6:** 751–759

Fonseca S, Chini A, Hamberg M, Adie B, Porzel A, Kramell R, Miersch O, Wasternack C, Solano R (2009) (+)-7-iso-Jasmonoyl-L-isoleucine is the endogenous bioactive jasmonate. Nat Chem Biol **5:** 344–350

He P, Chintamanani S, Chen Z, Zhu L, Kunkel BN, Alfano JR, Tang X, Zhou JM (2004) Activation of a COI1-dependent pathway in Arabidopsis by *Pseudomonas syringae* type III effectors and coronatine. Plant J **37:** 589–602

Ishiga Y, Uppalapati SR, Ishiga T, Elavarthi S, Martin B, Bender CL (2009) The phytotoxin coronatine induces light-dependent reactive oxygen species in tomato seedlings. New Phytol **181:** 147–160

Jander G, Norris SR, Rounsley SD, Bush DF, Levin IM, Last RL (2002) Arabidopsis map-based cloning in the post-genome era. Plant Physiol **129:** 440–450

Jiang H, Li M, Liang N, Yan H, Wei Y, Xu X, Liu J, Xu Z, Chen F, Wu G (2007) Molecular cloning and function analysis of the *stay green* gene in rice. Plant J **52:** 197–209

Katagiri F, Thilmony R, He SY (2002) *Arabidopsis thaliana-Pseudomonas syringae* interaction. The Arabidopsis Book. **1:** e0039, doi/10.1199/tab.0039

Katsir L, Schilmiller AL, Staswick PE, He SY, Howe GA (2008) COI1 is a critical component of a receptor for jasmonate and the bacterial virulence factor coronatine. Proc Natl Acad Sci USA **105:** 7100–7105

Kim JG, Taylor KW, Hotson A, Keegan M, Schmelz EA, Mudgett MB (2008) XopD SUMO protease affects host transcription, promotes pathogen growth, and delays symptom development in *xanthomonas*-infected tomato leaves. Plant Cell **20:** 1915–1929

Kloek AP, Verbsky ML, Sharma SB, Schoelz JE, Vogel J, Klessig DF, Kunkel BN (2001) Resistance to *Pseudomonas syringae* conferred by an *Arabidopsis thaliana* coronatine-insensitive (coi1) mutation occurs through two distinct mechanisms. Plant J **26:** 509–522

Laurie-Berry N, Joardar V, Street IH, Kunkel BN (2006) The *Arabidopsis thaliana JASMONATE INSENSITIVE 1* gene is required for suppression of salicylic acid-dependent defenses during infection by *Pseudomonas syringae*. Mol Plant Microbe Interact **19:** 789–800

Lewis JD, Guttman DS, Desveaux D (2009) The targeting of plant cellular systems by injected type III effector proteins. Semin Cell Dev Biol **20:** 1055–1063

Lorenzo O, Chico JM, Sánchez-Serrano JJ, Solano R (2004) *JASMONATE-INSENSITIVE1* encodes a MYC transcription factor essential to discriminate between different jasmonate-regulated defense responses in *Arabidopsis*. Plant Cell **16:** 1938–1950

Lukowitz W, Gillmor CS, Scheible WR (2000) Positional cloning in *Arabidopsis*: why it feels good to have a genome initiative working for you. Plant Physiol **123:** 795–805

Ma SW, Cuppels DA (1991) Characterization of a DNA region required for production of the phytotoxin coronatine by *Pseudomonas syringae* pv. *tomato*. Mol Plant Microbe Interact **4:** 69–77

Melotto M, Mecey C, Niu Y, Chung HS, Katsir L, Yao J, Zeng W, Thines B, Staswick P, Browse J, et al (2008a) A critical role of two positively charged amino acids in the Jas motif of Arabidopsis JAZ proteins in mediating coronatine- and jasmonoyl isoleucine-dependent interactions with the COI1 F-box protein. Plant J **55:** 979–988

Melotto M, Underwood W, He SY (2008b) Role of stomata in plant innate immunity and foliar bacterial diseases. Annu Rev Phytopathol **46:** 101–122

Melotto M, Underwood W, Koczan J, Nomura K, He SY (2006) Plant stomata function in innate immunity against bacterial invasion. Cell **126:** 969–980

Mendel G (1866) Versuche über pflanzen-hybriden. Verh Naturforsch Ver Brünn **4:** 3–47

Mittal S, Davis KR (1995) Role of the phytotoxin coronatine in the infection of *Arabidopsis thaliana* by *Pseudomonas syringae* pv. *tomato*. Mol Plant Microbe Interact **8:** 165–171

Mur LA, Aubry S, Mondhe M, Kingston-Smith A, Gallagher J, Timms-Taravella E, James C, Papp I, Hörtensteiner S, Thomas H, et al (2010) Accumulation of chlorophyll catabolites photosensitizes the hypersensitive response elicited by *Pseudomonas syringae* in Arabidopsis. New Phytol **188:** 161–174

Park SY, Yu JW, Park JS, Li J, Yoo SC, Lee NY, Lee SK, Jeong SW, Seo HS, Koh HJ, et al (2007) The senescence-induced staygreen protein regulates chlorophyll degradation. Plant Cell **19:** 1649–1664

Ren G, An K, Liao Y, Zhou X, Cao Y, Zhao H, Ge X, Kuai B (2007) Identification of a novel chloroplast protein AtNYE1 regulating chlorophyll degradation during leaf senescence in Arabidopsis. Plant Physiol **144:** 1429–1441

Sato Y, Morita R, Nishimura M, Yamaguchi H, Kusaba M (2007) Mendel's green cotyledon gene encodes a positive regulator of the chlorophyll-degrading pathway. Proc Natl Acad Sci USA **104:** 14169–14174

Sheard LB, Tan X, Mao H, Withers J, Ben-Nissan G, Hinds TR, Kobayashi Y, Hsu FF, Sharon M, Browse J, et al (2010) Jasmonate perception by inositol-phosphate-potentiated COI1-JAZ co-receptor. Nature **468:** 400–405

Thines B, Katsir L, Melotto M, Niu Y, Mandaokar A, Liu G, Nomura K, He SY, Howe GA, Browse J (2007) JAZ1 is a target of the SCF^{COI1} ubiquitin ligase during jasmonate signaling. Nature **448:** 661–665

Uppalapati SR, Ayoubi P, Weng H, Palmer DA, Mitchell RE, Jones W, Bender CL (2005) The phytotoxin coronatine and methyl jasmonate impact multiple phytohormone pathways in tomato. Plant J **42:** 201–217

Uppalapati SR, Ishiga Y, Ryu CM, Ishiga T, Wang K, Noël LD, Parker JE, Mysore KS (2011) SGT1 contributes to coronatine signaling and Pseu-

domonas syringae pv. tomato disease symptom development in tomato and Arabidopsis. New Phytol **189:** 83–93

Uppalapati SR, Ishiga Y, Wangdi T, Kunkel BN, Anand A, Mysore KS, Bender CL (2007) The phytotoxin coronatine contributes to pathogen fitness and is required for suppression of salicylic acid accumulation in tomato inoculated with *Pseudomonas syringae* pv. *tomato* DC3000. Mol Plant Microbe Interact **20:** 955–965

Whalen MC, Innes RW, Bent AF, Staskawicz BJ (1991) Identification of *Pseudomonas syringae* pathogens of *Arabidopsis* and a bacteriallocus determining avirulence on both *Arabidopsis* and soybean. Plant Cell **3:** 49–59

Yadav V, Mallappa C, Gangappa SN, Bhatia S, Chattopadhyay S (2005) A basic helix-loop-helix transcription factor in *Arabidopsis*, MYC2, acts as a repressor of blue light-mediated photomorphogenic growth. Plant Cell **17:** 1953–1966

Zeng W, He SY (2010) A prominent role of the flagellin receptor FLAGELLIN-SENSING2 in mediating stomatal response to *Pseudomonas syringae* pv tomato DC3000 in Arabidopsis. Plant Physiol **153:** 1188–1198